Title

A crucial role for HVEM and BTLA in preventing intestinal inflammation.

Journal

The Journal of experimental medicine, 205(6)

ISSN

0022-1007

Authors

Steinberg, Marcos W
Turovskaya, Olga
Shaikh, Raziya B
et al.

Publication Date

2008-06-01

DOI

10.1084/jem.20071160

Peer reviewed

A crucial role for HVEM and BTLA in preventing intestinal inflammation

Marcos W. Steinberg,[1] Olga Turovskaya,[1] Raziya B. Shaikh,[1] Gisen Kim,[1] Declan F. McCole,[3] Klaus Pfeffer,[4] Kenneth M. Murphy,[5] Carl F. Ware,[2] and Mitchell Kronenberg[1]

[1]Division of Developmental Immunology and [2]Division of Molecular Immunology, La Jolla Institute for Allergy and Immunology, La Jolla, CA 92037
[3]Division of Gastroenterology, Department of Medicine, University of California San Diego, School of Medicine, La Jolla, CA 92093
[4]Institute of Medical Microbiology, Heinrich-Heine-Universität Düsseldorf, D-40225 Düsseldorf, Germany
[5]Department of Pathology and Center for Immunology, and Howard Hughes Medical Institute, Washington University School of Medicine, St. Louis, MO 63110

The interaction between the tumor necrosis factor (TNF) family member LIGHT and the TNF family receptor herpes virus entry mediator (HVEM) co-stimulates T cells and promotes inflammation. However, HVEM also triggers inhibitory signals by acting as a ligand that binds to B and T lymphocyte attenuator (BTLA), an immunoglobulin super family member. The contribution of HVEM interacting with these two binding partners in inflammatory processes remains unknown. In this study, we investigated the role of HVEM in the development of colitis induced by the transfer of $CD4^+CD45RB^{high}$ T cells into recombination activating gene $(Rag)^{-/-}$ mice. Although the absence of HVEM on the donor T cells led to a slight decrease in pathogenesis, surprisingly, the absence of HVEM in the $Rag^{-/-}$ recipients led to the opposite effect, a dramatic acceleration of intestinal inflammation. Furthermore, the critical role of HVEM in preventing colitis acceleration mainly involved HVEM expression by radioresistant cells in the $Rag^{-/-}$ recipients interacting with BTLA. Our experiments emphasize the antiinflammatory role of HVEM and the importance of HVEM expression by innate immune cells in preventing runaway inflammation in the intestine.

CORRESPONDENCE
Mitchell Kronenberg:
mitch@liai.org

Abbreviations used: BTLA, B and T lymphocyte attenuator; DSS, dextran sodium sulfate; GVHD, graft versus host disease; H&E, hematoxylin and eosin; HVEM, herpes virus entry mediator; IBD, inflammatory bowel disease; IEC, intestinal epithelial cell; IEL, intestinal epithelial lymphocyte; LPL, lamina propria lymphocyte; MLN, mesenteric lymph node.

Inflammatory bowel diseases (IBDs) comprise a spectrum of immune-mediated conditions in which the target organ is the intestine. IBD is divided into two primary forms, Crohn's disease and ulcerative colitis (1). Although the etiology remains unknown, increasing evidence suggests that IBD is the result of a dysregulated mucosal inflammatory response (2). TNF is a particularly important contributor to intestinal inflammation, and blockade of TNF with anti-TNF antibodies is an effective treatment for a subset of Crohn's disease patients (3). Several lines of evidence point to the TNF-related cytokine LIGHT (homologous to lymphotoxin, shows inducible expression, and competes with HSV glycoprotein D for herpes virus entry mediator [HVEM], a receptor expressed by T lymphocytes) as another important mediator of mucosal inflammation and IBD pathogenesis (4–6). Activated T cells and immature DCs express LIGHT, and it has been described as a proinflammatory cytokine and a potent T cell co-stimulatory molecule (7–10). Mature Th1-type $CD4^+$ T cells and mucosal T cells isolated from patients with IBD express high levels of LIGHT (4). Furthermore, transgenic mice with T cells constitutively expressing LIGHT developed spontaneous multi-organ inflammation that included the intestine (11, 12), and intestinal inflammation could be induced by transfer of LIGHT transgenic T cells (13).

LIGHT signals via two members of the TNF receptor super family, the lymphotoxin β receptor, predominantly expressed by myeloid lineage, stromal, and epithelial cells (14–17), and the HVEM, broadly expressed by hematopoietic cells as well as by some somatic cells (18–21). LIGHT-mediated IBD pathogenesis in mice has been attributed to its interaction with both of these receptors (6). Whereas the interaction of LIGHT with lymphotoxin β receptor is thought to induce transformations in

The online version of this article contains supplemental material.

The Rockefeller University Press $30.00
J. Exp. Med. Vol. 205 No. 6 1463-1476 www.jem.org/cgi/doi/10.1084/jem.20071160

The Journal of Experimental Medicine

the gut mucosa that alter the normal microenvironment of the intestine, its binding with HVEM expressed by T cells promotes T cell activation and the T cell expansion required for the full development of disease (6). In other contexts, engagement of HVEM by LIGHT delivers co-stimulatory signals leading to T cell activation (8, 9, 18, 22) and enhanced T cell–mediated immunity (11, 12, 19, 23, 24). Furthermore, it has been described that engagement of HVEM by LIGHT induced activation of human mucosal T cells and increased IFN-γ release (4). Therefore, it appears that HVEM may contribute to IBD pathogenesis by promoting T cell activation and Th1 responses (4, 6).

It has been recently discovered, however, that HVEM can also deliver inhibitory signals to T cells (25, 26). These inhibitory signals involve a receptor that binds HVEM, a member of the Ig super family called B and T lymphocyte attenuator (BTLA) (25). Once engaged by HVEM, the ITIM motifs in the cytoplasmic tail of BTLA become tyrosine phosphorylated, allowing the recruitment of the phosphatases SHP-1 and SHP-2 (27, 28). Recent studies have shown that HVEM- as well as BTLA-deficient T cells are hyperresponsive to TCR-induced stimulation in vitro (26–28). Additionally, both HVEM- and BTLA-deficient mice presented a higher susceptibility to experimental autoimmune encephalomyelitis (26, 28), whereas the loss of BTLA dramatically accelerated partially MHC-mismatched cardiac allograft rejection (29) and prolonged airway inflammation (30). Furthermore, the BTLA–HVEM interaction limited T cell activity in vivo, negatively regulating the homeostatic expansion of a subset of $CD8^+$ memory T cells (31). Despite its generally inhibitory role, BTLA has recently been reported to play a role in promoting the survival of T cells activated during a mouse model of graft versus host disease (GVHD) (32).

Therefore, whereas some evidence indicates that HVEM is the co-stimulatory receptor responsible for LIGHT-mediated T cell activation, other data demonstrate that HVEM can be a negative regulator of T cell responses by triggering BTLA-derived inhibitory signals. The actual contribution of HVEM to T cell–mediated immune responses, and to the pathogenesis of T cell–mediated inflammatory conditions such as IBD, remains to be determined. Moreover, most of the studies that investigate the role of HVEM binding to its ligands have emphasized the expression of one or more of these molecules by B and T lymphocytes, and their roles in directly regulating lymphocyte responses. In this study, we investigated the role of HVEM and its binding partners in the development of colitis induced by the transfer of $CD4^+CD45RB^{high}$ T cells into $Rag^{-/-}$ mice, and the possible function of HVEM in cells of the innate immune system that are present in the $Rag^{-/-}$ hosts.

RESULTS

The role of HVEM expression by T cells in colitis induction

To investigate the participation of HVEM in colitis pathogenesis, we used an experimental mouse model initiated by the adoptive transfer of $CD4^+CD45RB^{high}$ naive T cells, depleted of $CD25^+$ regulatory T cells, into syngeneic $Rag^{-/-}$ mice. This leads to a progressive disease, with weight loss and colitis appearing 5–10 wk after the transfer (33). To evaluate if the expression of HVEM in T cells is required for colitis induction, we transferred $CD4^+CD45RB^{high}$ T cells isolated from $Hvem^{-/-}$ or WT mice into $Rag^{-/-}$ recipients. As expected, WT donor $CD4^+CD45RB^{high}$ T cells induced a gradual weight loss in $Rag^{-/-}$ recipients that correlated with disease progression, as did the transfer of $Hvem^{-/-}$ $CD4^+CD45RB^{high}$ T cells (Fig. 1 A). Although at early time points after the transfer weight loss in the $Rag^{-/-}$ recipient mice of $Hvem^{-/-}$ T cells was slightly less pronounced, the recipients

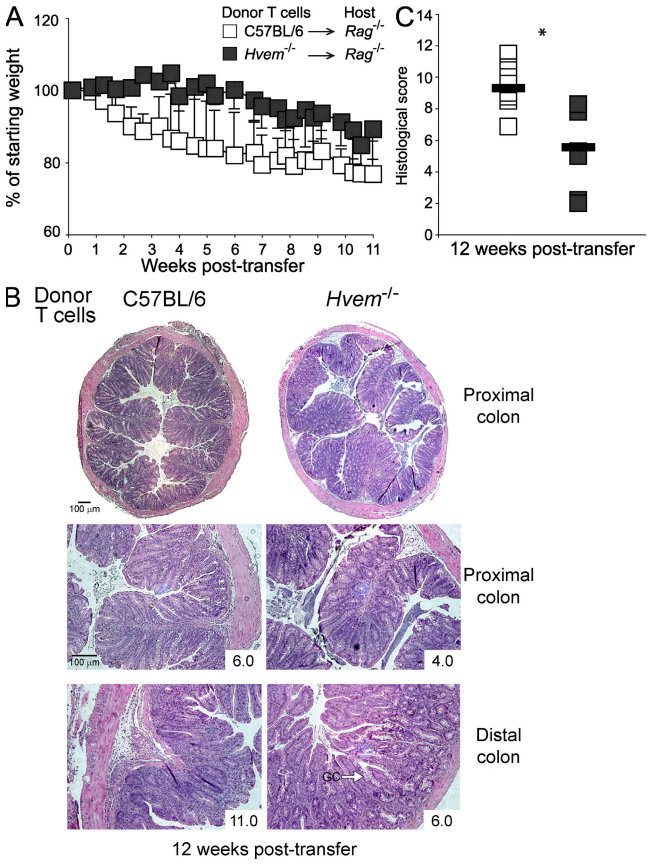

Figure 1. $CD4^+CD45RB^{high}$ T cells do not require HVEM to induce colitis. (A) Weight loss curves of $Rag^{-/-}$ recipients transferred with 5×10^5 $CD4^+CD45RB^{high}$ T cells isolated from either WT C57BL/6 mice (open squares) or $Hvem^{-/-}$ mice (filled squares). The graph shows the average weight loss as a percentage of the initial weight of four mice in each group, and they are representative of four independent experiments. (B) H&E staining of proximal and distal colon of $Rag^{-/-}$ mice transferred with WT or $Hvem^{-/-}$ T cells. The histological scores of the representative sections shown are indicated (bottom right of each panel). GC, goblet cells. (C) Average scores of the proximal and distal colon sections were evaluated 12 wk after the transfer of T cells. Sections of the large intestine isolated from different recipients were microscopically analyzed as described in Materials and methods. Each square represents a single mouse (eight per group). *, $P < 0.05$.

unquestionably became ill, eventually all the transferred *Rag*$^{-/-}$ recipients showed an equivalent weight loss (Fig. 1 A), and the overall difference between *Hvem*$^{-/-}$ and WT donor T cells did not reach statistical significance. Microscopic analysis of hematoxylin and eosin (H&E)-stained tissue sections obtained from the large intestine of transferred mice revealed severe inflammation in all of the recipients. However, mice transferred with *Hvem*$^{-/-}$ T cells had lower mononuclear cell infiltrates in the proximal and distal colon. In addition, these recipients had a higher number of goblet cells in the distal colon, indicating that inflammation in these animals was milder (Fig. 1 B). Scoring of sections obtained from the recipients transferred with *Hvem*$^{-/-}$ T cells showed a lower average histological score than in the animals that received WT T cells (Fig. 1 C). Overall, these results suggest that HVEM expression on donor T cells contributed to a limited extent to increasing intestinal inflammation; however, HVEM expression in T cells was not absolutely required for colitis development.

Accelerated colitis in *Hvem*$^{-/-}$*Rag*$^{-/-}$ recipients

HVEM expression is not restricted to T cells, and therefore to evaluate if HVEM expressed by non–T cells participates in colitis pathogenesis, we bred HVEM-deficient *Rag*$^{-/-}$ (*Hvem*$^{-/-}$*Rag*$^{-/-}$) animals to use as recipients. *Hvem*$^{-/-}$*Rag*$^{-/-}$ recipients that were transferred with WT CD4^{+}CD45RB^{high} T cells exhibited a surprising acceleration of weight loss and colitis, as determined by the presence of diarrhea and other clinical signs, such as reduced mobility and piloerection of the fur. Notably, recipient *Hvem*$^{-/-}$*Rag*$^{-/-}$ mice showed a reduction of ~20% of their initial starting weight only 2 wk after transfer (Fig. 2 A). The intestinal inflammation in these recipients was progressive and lethal, and in most cases the recipients did not survive beyond 3–4 wk after transfer. This accelerated inflammation was confined, however, predominantly to the large intestine (not depicted). Conversely, in the same brief period, *Rag*$^{-/-}$ recipients did not show any weight loss (Fig. 2 A). In addition to the faster weight loss, transferred *Hvem*$^{-/-}$*Rag*$^{-/-}$ mice presented early evidence of

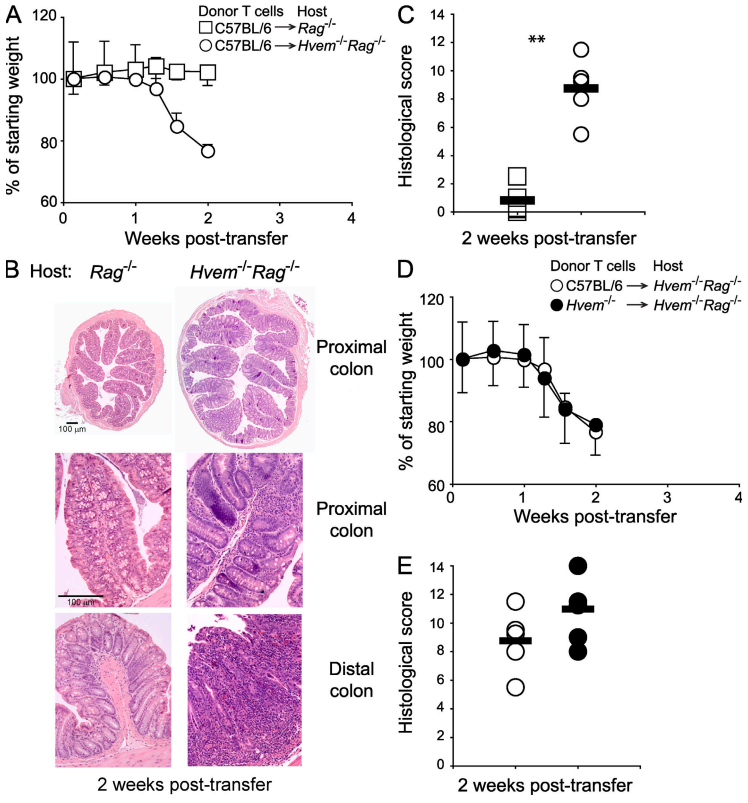

Figure 2. Colitis acceleration in *Hvem*$^{-/-}$*Rag*$^{-/-}$ mice. Transfer of CD4^{+}CD45RB^{high} T cells into *Hvem*$^{-/-}$*Rag*$^{-/-}$ mice dramatically accelerated colitis. (A) Weight loss curves of *Rag*$^{-/-}$ (squares) and *Hvem*$^{-/-}$*Rag*$^{-/-}$ (circles) recipients of 5 × 10^{5} WT T cells showed an extremely rapid disease progression in *Hvem*$^{-/-}$*Rag*$^{-/-}$ animals. Data correspond to the average of five mice per group and are representative of five independent experiments. (B) H&E staining of proximal and distal colon sections are shown. (C) Average scores of the proximal and distal colon sections from individual mice were evaluated 2 wk after the transfer of T cells. Each symbol represents an individual mouse (n = 5), and representative data from four experiments are shown. **, $P < 0.005$. (D) Weight loss comparison after transfer of WT (open circles) or *Hvem*$^{-/-}$ (filled circles) CD4^{+}CD45RB^{high} T cells into *Hvem*$^{-/-}$*Rag*$^{-/-}$ recipients (n = 6–7). (E) Combined proximal and distal histological analysis of colon sections performed 2 wk after the transfers described in part D. Each symbol represents an individual mouse (n = 7).

severe intestinal inflammation. Examination of H&E-stained sections obtained from *Hvem*$^{-/-}$*Rag*$^{-/-}$ recipients revealed prominent epithelial cell hyperplasia, absence of goblet cells, and a massive infiltration of mononuclear cells in the colons of these animals (Fig. 2 B). Histological analysis performed on samples isolated from large intestine of these recipients 2 wk after transfer had an average pathology score of 8.8 ± 2.2 out of a possible of 14 (Fig. 2 C). Samples from *Rag*$^{-/-}$ recipients at the same early time after transfer showed almost intact epithelial crypts with absence of epithelial cell hyperplasia and only few mononuclear cell infiltrates (Fig. 2 B). The average score for samples obtained from the transferred *Rag*$^{-/-}$ mice at this time was only 0.8 ± 1.0 (Fig. 2 C).

We transferred *Hvem*$^{-/-}$ donor T cells into *Hvem*$^{-/-}$*Rag*$^{-/-}$ mice to analyze the situation in which HVEM is entirely missing. Interestingly, induced colitis and wasting disease in the completely HVEM-deficient situation were still accelerated compared with transfers to *Rag*$^{-/-}$ animals. Weight loss in *Hvem*$^{-/-}$*Rag*$^{-/-}$ mice transferred with HVEM-deficient T cells was equally accelerated compared with the same recipients transferred with WT T cells (Fig. 2 D). Histological scores in these recipients completely lacking HVEM were also equivalent to those observed in *Hvem*$^{-/-}$*Rag*$^{-/-}$ animals transferred with WT T cells (Fig. 2 E). Overall, these results demonstrate that the absence of HVEM expression in *Rag*$^{-/-}$ host cells led to a dramatic acceleration of colitis, and they show that this dramatic effect was dominant over any deceleration of disease caused by the absence of HVEM expression by donor T cells.

Rapid accumulation of T cells in the large intestine of *Hvem*$^{-/-}$*Rag*$^{-/-}$ recipients

To characterize the colitis acceleration observed in *Hvem*$^{-/-}$*Rag*$^{-/-}$ mice, we investigated the fate of the transferred T cells. We determined the number of CD4$^+$ T lymphocytes in the spleens and mesenteric lymph nodes (MLNs) of transferred mice, two sites where T cells expand dramatically after transfer to immune-deficient hosts (34, 35). 1 wk after transfer, the number of CD4$^+$ T cells in the MLNs of *Hvem*$^{-/-}$*Rag*$^{-/-}$ animals was approximately threefold higher than in *Rag*$^{-/-}$ mice (Fig. 3 A). This difference was highly significant ($P = 0.005$). The number of T cells in the spleens of *Hvem*$^{-/-}$*Rag*$^{-/-}$ mice was also slightly higher than in *Rag*$^{-/-}$ recipients, although not statistically significant (Fig. 3 A). Elevated numbers of T cells in the MLNs of *Hvem*$^{-/-}$*Rag*$^{-/-}$ animals were only observed at early time points after the transfer, and by 2 wk after transfer, the number of CD4$^+$ TCR-β$^+$ lymphocytes in the MLNs was essentially equivalent in both recipients (Fig. 3 B). To investigate if the early accumulation of transferred T cells in inductive sites such as MLNs in the *Hvem*$^{-/-}$*Rag*$^{-/-}$ mice also affected the target organ, we assessed the accumulation of CD4$^+$ TCR-β$^+$ T cells in the large intestine of the recipients. As early as 7 d after transfer, T lymphocytes were detectable in the large intestine. At this time, the average number of CD4$^+$ TCR-β$^+$ cells infiltrating the epithelium of the *Hvem*$^{-/-}$*Rag*$^{-/-}$ mice was 2.3-fold higher than in *Rag*$^{-/-}$ mice (Fig. 3 A). However, by 2 wk after transfer, intraepithelial CD4$^+$ TCR-β$^+$ cell numbers in *Hvem*$^{-/-}$*Rag*$^{-/-}$ mice were 10-fold higher ($P < 0.005$) (Fig. 3 B). Accordingly, the number of CD4$^+$ TCR-β$^+$ lamina propria lymphocytes (LPLs) was also significantly higher in *Hvem*$^{-/-}$*Rag*$^{-/-}$ recipients at 2 wk (Fig. 3 B). Collectively, these results demonstrate that the absence of HVEM in the *Rag*$^{-/-}$ mice led to a more rapid accumulation of transferred T cells in the MLNs and large intestine.

Increased T cell cytokine production in *Hvem*$^{-/-}$*Rag*$^{-/-}$ recipients

To further characterize the colitis acceleration observed in *Hvem*$^{-/-}$*Rag*$^{-/-}$ mice, we investigated the profile of cytokines produced in the large intestine of the recipient animals. 2 wk after transfer, total mRNA was purified from the colon and subjected to RT-PCR analysis for several cytokines. RT-PCR revealed the presence of TNF and IFN-γ mRNAs, and lower levels of IL-17 mRNA (Fig. 3 C). Notably, the amount of mRNA for these cytokines, and in particular for TNF, was considerably higher in samples isolated from *Hvem*$^{-/-}$*Rag*$^{-/-}$ mice (Fig. 3 C). The higher level of proinflammatory cytokines in the intestine of *Hvem*$^{-/-}$*Rag*$^{-/-}$ animals correlated with the rapid and severe intestinal inflammation observed. It should be noted that increased mRNA for TGF-β and IL-10 in the *Hvem*$^{-/-}$*Rag*$^{-/-}$ mice was also observed when compared with *Rag*$^{-/-}$ recipients. The increased presence of these antiinflammatory cytokine mRNAs in the *Hvem*$^{-/-}$*Rag*$^{-/-}$ recipients could reflect a compensatory regulatory mechanism in the face of inflammation, although the amount of IL-10 mRNA was very low in all the samples (Fig. 3 D). The amount of mRNA for IL-12 family cytokines in the colon was not very great, but in accord with the higher levels of IFN-γ mRNA observed in *Hvem*$^{-/-}$*Rag*$^{-/-}$ mice, we also detected an increase in IL-12 mRNA in the colon of these animals (Fig. 3 E). The level of mRNA for IL-23, however, was equivalent in both *Rag*$^{-/-}$ and *Hvem*$^{-/-}$*Rag*$^{-/-}$ mice (Fig. 3 E).

To determine if the transferred T cells had the capacity to produce proinflammatory cytokines in the colon of the *Hvem*$^{-/-}$*Rag*$^{-/-}$ recipient mice, we evaluated cytokine production by donor-derived LPLs restimulated in vitro. LPLs were purified from the large intestine of *Rag*$^{-/-}$ or *Hvem*$^{-/-}$*Rag*$^{-/-}$ recipient mice, stimulated with PMA, and ionomycin, and 48 h later cytokines were determined by ELISA. The amounts of IFN-γ, TNF, and IL-2 in the culture supernatants of cells obtained from *Hvem*$^{-/-}$*Rag*$^{-/-}$ mice were considerably higher than those secreted by cells isolated from *Rag*$^{-/-}$ recipients (Fig. 3 F). Rather than an increased capacity to produce cytokines, the higher amounts of cytokines in the cultures of cells isolated from *Hvem*$^{-/-}$*Rag*$^{-/-}$ mice could have been due to the increased number of T cells in the LPL preparations. Indeed, the percentage of CD4$^+$ TCR-β$^+$ within the LPL suspension isolated from *Hvem*$^{-/-}$*Rag*$^{-/-}$ mice was about twofold higher than that observed in *Rag*$^{-/-}$ animals (not depicted). The increment in cytokines in the isolated LPLs from *Hvem*$^{-/-}$*Rag*$^{-/-}$ mice was increased more than twofold,

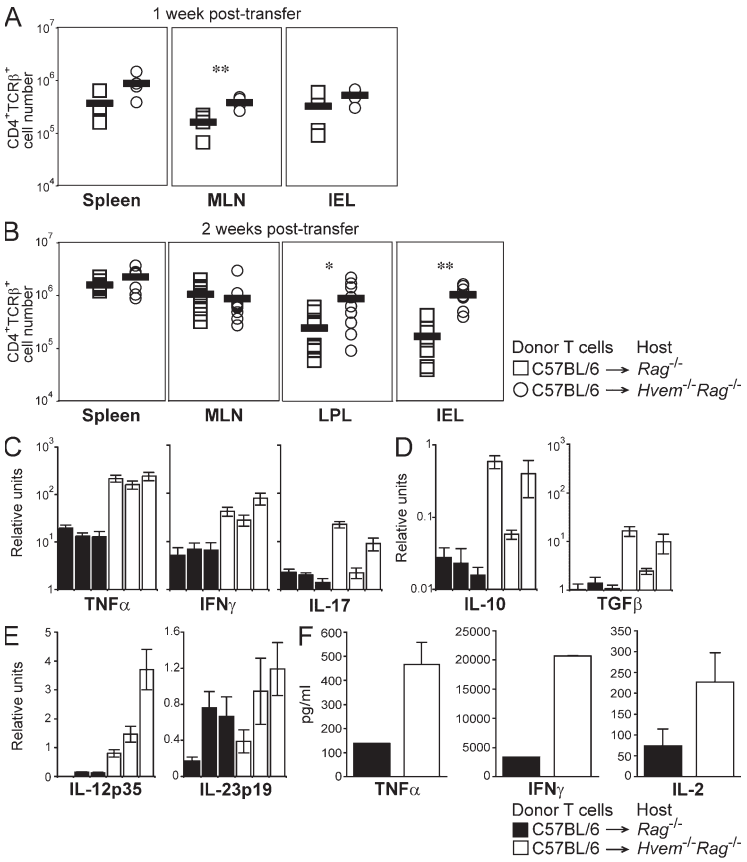

Figure 3. Increased T cells and cytokines in *Hvem*$^{-/-}$*Rag*$^{-/-}$ recipients. The number of CD4+ TCR-β+ cells in the spleens, MLNs, and large intestines of recipient mice was assessed at the indicated times. (A) 1 wk after transfer, *Rag*$^{-/-}$ (squares) and *Hvem*$^{-/-}$*Rag*$^{-/-}$ (circles) mice, four in each group, were analyzed by flow cytometry for T cells in the spleens, large IELs, and MLNs. (B) Shows same as in A, but including LPLs and analyzed 2 wk after transfer. Each symbol represents an individual mouse with a total of 7–10 mice per group. *, $P < 0.05$; **, $P < 0.005$. (C–E) Real-time PCR performed on tissue samples isolated from the large intestines of individual *Rag*$^{-/-}$ (filled bars) or *Hvem*$^{-/-}$*Rag*$^{-/-}$ (open bars) recipients 2 wk after transfer. Error bars represent SD of triplicate measurements. (F) LPLs isolated from transferred *Hvem*$^{-/-}$*Rag*$^{-/-}$ (open bars) and *Rag*$^{-/-}$ (filled bars) recipients at 2 wk were stimulated ex vivo with PMA and ionomycin. After 48 h, cytokines in the supernatant were measured by ELISA.

however, suggesting that increased proinflammatory cytokines in the LPLs of these recipients could be due to a combination of increased cell number and increased effectors. Collectively, these findings suggest that the presence of increased CD4+ T cells secreting high amounts of proinflammatory cytokines in the intestine of *Hvem*$^{-/-}$*Rag*$^{-/-}$ recipients contributed to the more rapid development of colitis.

DCs were not greatly affected in *Hvem*$^{-/-}$ mice

Previous reports have suggested a role for HVEM in DC maturation and cytokine production (36, 37), and therefore the absence of HVEM expression on DCs in the *Rag*$^{-/-}$ recipients might cause an abnormal development and/or function of these cells. In WT or *Hvem*$^{-/-}$ mice, however, the percentage of DCs in the spleens and MLNs was essentially equivalent, and the two major subsets of DCs, those expressing high levels of CD11c and CD8α, and those expressing CD11b, were similarly represented in the MLNs of WT and *Hvem*$^{-/-}$ animals (Fig. S1 A, available at http://www.jem.org/cgi/content/full/jem.20071160/DC1, and not depicted). CD11c+ cells freshly isolated from the MLNs of the two types of mice expressed equivalent levels of the co-stimulatory molecules CD86 and CD80, suggesting that the DC maturation state was not greatly affected by the absence of HVEM (Fig. S1 A). To determine if the threshold for stimulation for DCs is altered in the absence of HVEM, CD11c+ cells from MLNs were stimulated with LPS. Upon stimulation, both WT and *Hvem*$^{-/-}$ DCs expressed similar levels of CD40 and CD86 (Fig. S1 B). Moreover, after LPS stimulation, the percentage of WT and *Hvem*$^{-/-}$ MLN DCs expressing IL-12 was essentially equivalent (Fig. S1 B). Collectively, these results demonstrate that the absence of HVEM in DCs did not significantly affect their percentage, maturation state, or their capacity to secrete cytokines. For priming naive CD4+ T cells, freshly isolated DCs from the MLNs of *Hvem*$^{-/-}$ mice were slightly more effective than their WT counterparts (proliferation indices of 2.6 and 2.1, respectively), although splenic DCs from these mice were not different from WT mice (Fig. S1 C). Likewise MLN DCs from mice deficient for the HVEM ligand BTLA did not prime more

effectively (Fig. S1 C). In summary, HVEM deficiency did not grossly alter DCs, and the small increase in proliferation of naive T cells stimulated with *Hvem*$^{-/-}$ DCs from MLNs is unlikely to account by itself for the accelerated T cell expansion and colitis pathogenesis in *Hvem*$^{-/-}$ recipients.

HVEM expression in radioresistant cells is required to prevent colitis acceleration

Because there was not an obvious APC defect in the *Hvem*$^{-/-}$ mice, to begin to identify the critical cell type(s) that must express HVEM, we analyzed chimeric *Rag*$^{-/-}$ recipient mice that expressed HVEM only in irradiation-resistant cells, or only in cells derived from BM progenitors. To construct the chimeras, after lethal irradiation, *Hvem*$^{-/-}$*Rag*$^{-/-}$ mice were reconstituted with *Rag*$^{-/-}$ BM cells (*Rag*$^{-/-}$→*Hvem*$^{-/-}$*Rag*$^{-/-}$), and reciprocal chimeras were constructed in *Rag*$^{-/-}$ mice given *Hvem*$^{-/-}$*Rag*$^{-/-}$ BM cells (*Hvem*$^{-/-}$*Rag*$^{-/-}$→*Rag*$^{-/-}$) (Fig. 4 A). To verify that the chimeric mice were properly reconstituted, 8 wk after BM transplantation HVEM expression in peripheral blood cells from these animals was monitored. As expected, blood cells isolated from *Hvem*$^{-/-}$*Rag*$^{-/-}$→*Rag*$^{-/-}$ mice expressing the hematopoietic lineage marker CD45 did not have detectable surface HVEM, indicating reconstitution by the *Hvem*$^{-/-}$ donor BM cells (Fig. 4 B). In contrast, in *Rag*$^{-/-}$→*Hvem*$^{-/-}$*Rag*$^{-/-}$ chimeric mice the vast majority of the hematopoietic cells expressed intermediate or high levels of HVEM, indicating that they derived from the *Hvem*$^{+/+}$ donors (Fig. 4 B). A similar degree of reconstitution was observed when organs containing immune cells from the chimeras were analyzed (not depicted).

Surprisingly, the transfer of CD4^{+}CD45RB^{high} T cells into *Rag*$^{-/-}$→*Hvem*$^{-/-}$*Rag*$^{-/-}$ chimeric recipients induced a

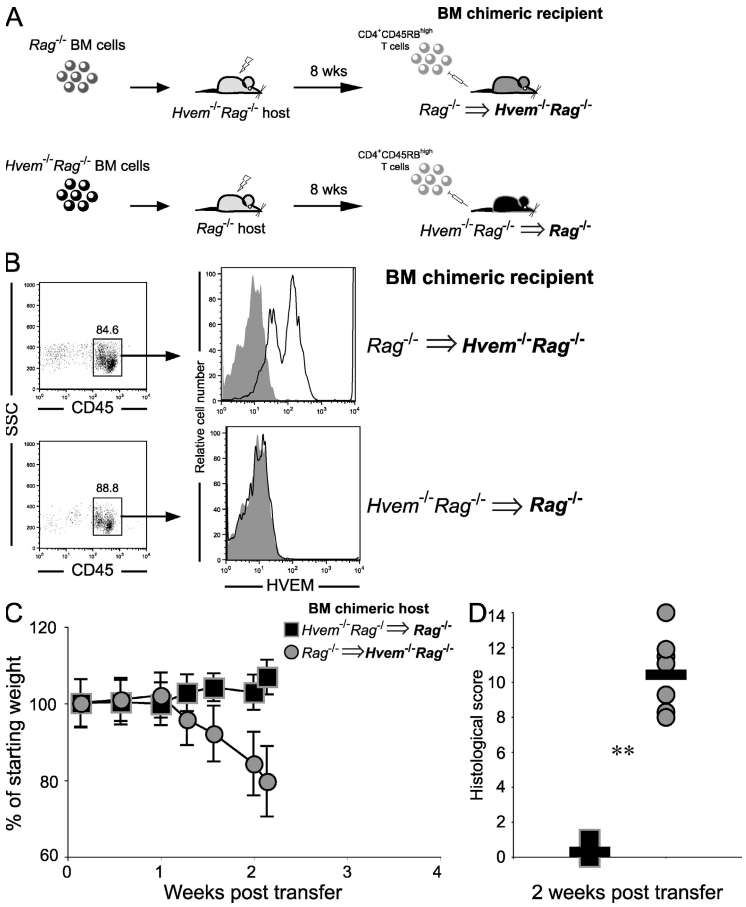

Figure 4. HVEM expression by radioresistant *Rag*$^{-/-}$ cells prevents colitis acceleration. (A) Experimental design. Lethally irradiated *Hvem*$^{-/-}$*Rag*$^{-/-}$ mice were transplanted with *Rag*$^{-/-}$ BM cells to generate *Rag*$^{-/-}$→*Hvem*$^{-/-}$*Rag*$^{-/-}$ chimeric mice. Reciprocal *Hvem*$^{-/-}$*Rag*$^{-/-}$→*Rag*$^{-/-}$ chimeras also were generated. 10 wk after transplant, chimeric mice were used as recipients of CD4^{+}CD45RB^{high} T cells. (B) Analysis of reconstitution. HVEM expression in peripheral blood cells of the chimeric animals was assessed 8 wk after BM cell transplant by flow cytometry analysis for HVEM expression by CD45^{+} cells. Open histograms represent HVEM staining, and filled histograms represent the isotype control. Representative data are shown from one of many similar analyses of blood cells and cells from immune organs. (C) Transfer of 5 × 10^{5} CD4^{+}CD45RB^{high} T cells into *Hvem*$^{-/-}$*Rag*$^{-/-}$→*Rag*$^{-/-}$ (squares) and *Rag*$^{-/-}$→*Hvem*$^{-/-}$*Rag*$^{-/-}$ (gray circles) chimeric recipients. Weight loss curves correspond to the average of six to eight chimeric mice per group. (D) Histological scores were determined 2 wk after transfer. Each symbol represents a single mouse of a total of seven *Hvem*$^{-/-}$*Rag*$^{-/-}$→*Rag*$^{-/-}$ (squares) and eight *Rag*$^{-/-}$→*Hvem*$^{-/-}$*Rag*$^{-/-}$ (circles) chimeric mice. **, $P < 0.005$. Data shown are representative from one of two independent experiments.

rapidly developing disease (Fig. 4 C). Similar to the intact *Hvem*$^{-/-}$*Rag*$^{-/-}$ mice, *Rag*$^{-/-}$→*Hvem*$^{-/-}$*Rag*$^{-/-}$ recipients lost >20% of their initial weight by 2 wk after T cell transfer. Conversely, *Hvem*$^{-/-}$*Rag*$^{-/-}$→*Rag*$^{-/-}$ chimeric recipients that received CD4^{+}CD45RB^{high} T lymphocytes did not lose body weight in the same period of time (Fig. 4 C). Consistent with the difference in weight loss, histological scoring performed in large intestine samples collected from the transferred chimeric recipients revealed a more severe inflammation and tissue damage in *Rag*$^{-/-}$→*Hvem*$^{-/-}$*Rag*$^{-/-}$ mice than in the *Hvem*$^{-/-}$*Rag*$^{-/-}$→*Rag*$^{-/-}$ recipients (average score = 10.4 ± 2.0 in *Rag*$^{-/-}$→*Hvem*$^{-/-}$*Rag*$^{-/-}$ animals as opposed to 0.3 ± 0.5 in *Hvem*$^{-/-}$*Rag*$^{-/-}$→*Rag*$^{-/-}$ mice) (Fig. 4 D). These results indicate that HVEM prevents colitis acceleration principally when expressed by radioresistant cells in the *Rag*$^{-/-}$ hosts.

A radiation-resistant cell that might prevent accelerated inflammation through HVEM expression is the intestinal epithelial cell (IEC). In fact, human epithelial carcinoma cell lines (not depicted) and freshly isolated mouse colonic epithelial cells express HVEM (Fig. S2 A, available at http://www.jem.org/cgi/content/full/jem.20071160/DC1). A feature of IBD, in particular Crohn's disease, is increased intestinal permeability arising from a defect in the intestinal epithelium. Permeability to D-[1-^{14}C]-mannitol therefore was measured across tissues from proximal and distal large intestine, as well as the cecum, which were stripped of underlying smooth muscle and mounted in Ussing chambers. Although the trend was toward increased permeability in the distal colon of *Hvem*$^{-/-}$ mice, the difference was not significant when compared with WT tissues. However, permeability in the distal colon of both WT and *Hvem*$^{-/-}$ mice was significantly lower than that observed in inflamed tissues isolated from WT mice with colitis that had been induced by dextran sodium sulfate (DSS) (Fig. S2 B). Similar to the results from the distal large intestine, permeability in the proximal colon and cecum of WT and *Hvem*$^{-/-}$ animals was essentially equivalent (not depicted). Therefore, epithelial permeability is not compromised under noninflammatory conditions in the absence of HVEM expression. Colitis induced by DSS represents a well-established epithelial injury model of intestinal inflammation. *Hvem*$^{-/-}$ mice also displayed no increase in susceptibility to DSS-induced colitis when compared with WT mice (Fig. S3, A and B).

Effects of HVEM ligand expression by T cells

An appealing hypothesis for explaining the accelerated colitis in *Hvem*$^{-/-}$*Rag*$^{-/-}$ recipients is that enhanced disease is caused by the absence of an interaction between HVEM expressed by a cell type in the *Rag*$^{-/-}$ recipients with an HVEM binding partner expressed by the donor T cells. Recent publications have suggested that expression of LIGHT by T cells is able to regulate innate immune responses by interacting with the HVEM receptor (36, 38–41). Therefore, the absence of interactions between T cell–derived LIGHT and HVEM on host cells might lead to a dysregulated innate immune response in *Rag*$^{-/-}$ animals and accelerated development of disease. We therefore performed transfer experiments using *Light*$^{-/-}$ donor T cells. The results showed similar weight loss in *Rag*$^{-/-}$ mice transferred with either *Light*$^{-/-}$ or WT CD4^{+}CD45RB^{high} T cells (Fig. 5 A). However, histological analysis performed in samples obtained from the large intestine of *Rag*$^{-/-}$ recipients 12 wk after the transfer revealed lower levels of inflammation in animals transferred with *Light*$^{-/-}$ T cells (Fig. 5 B). This is consistent with other data indicating that LIGHT is a co-stimulatory molecule for T lymphocytes. Because the outcome after transfer of *Light*$^{-/-}$ T cells was opposite to the results after transfer to *Hvem*$^{-/-}$*Rag*$^{-/-}$ recipients, we conclude that the accelerating effects of host HVEM deficiency were not due to the absence of interactions with LIGHT expressed by the donor T cells.

Importantly, the transfer of *Light*$^{-/-}$ CD4^{+}CD45RB^{high} T cells into *Hvem*$^{-/-}$*Rag*$^{-/-}$ recipients induced a dramatic acceleration of weight loss (Fig. 5 C) and colitis progression assessed by the presence of diarrhea and other clinical signs. The disease acceleration was similar to that observed in *Hvem*$^{-/-}$*Rag*$^{-/-}$ mice transferred with WT T cells. Furthermore, the histological scores obtained with samples isolated from these *Hvem*$^{-/-}$*Rag*$^{-/-}$ animals 2 wk after the transfer showed equivalent levels of intestinal inflammation, regardless of the presence of LIGHT expression by the donor T cells (Fig. 5 D).

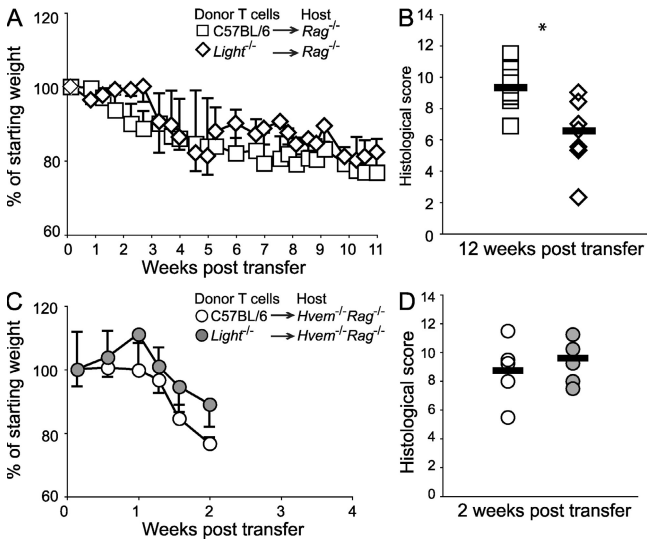

Figure 5. *Light*$^{-/-}$ T cells do not cause accelerated colitis. (A) Weight loss curves of *Rag*$^{-/-}$ recipients transferred with either WT (open squares) or *Light*$^{-/-}$ CD4^{+}CD45RB^{high} T cells (open diamonds). The graph shows the average of four mice per group and is representative of one of three independent experiments. (B) Average histological scores were evaluated 12 wk after T cell transfer. Each square represents a single mouse of a total of six to seven mice in each group. *, $P < 0.05$. (C) Results from the transfer of either WT (open circles) or *Light*$^{-/-}$ (filled circles) T cells into *Hvem*$^{-/-}$*Rag*$^{-/-}$ mice. Data shown correspond to the average weight loss of six mice per group. (D) Average histological scores analyzed 2 wk after WT or *Light*$^{-/-}$ CD4^{+}CD45RB^{high} T cell transfer to *Hvem*$^{-/-}$*Rag*$^{-/-}$ animals. Each circle represents a single mouse in a total of six mice per group.

Therefore, rapid colitis induction in the absence of HVEM expression is dominant over the decreased inflammation observed when *Light*$^{-/-}$ T cells were transferred.

The inhibitory HVEM ligand BTLA is expressed by activated T cells, and therefore interactions between *Rag*$^{-/-}$ host HVEM and T cell BTLA could alter the acceleration of colitis. To test this, we evaluated BTLA expression by naive CD4$^+$ T cells and by CD4$^+$ T cells after transfer. Consistent with previous reports (42), we detected BTLA expression on naive and activated CD4$^+$ T lymphocytes. In vitro TCR stimulation enhanced BTLA expression on CD4$^+$ T cells, with the highest level of BTLA observed 2–3 d after stimulation (Fig. 6 A). Likewise, we found BTLA expression on CD4$^+$ T cells isolated from the spleens, MLNs, and LPLs of transferred *Rag*$^{-/-}$ recipients (Fig. 6 B). Although BTLA expression on LPLs was slightly lower than that observed on T cells from the spleens or MLNs, this was likely a consequence of the reduced surface protein expression caused by the collagenase digestion during LPL isolation. Consistent with this, the amount of CD4 was also reduced (mean fluorescence intensity = 7,456 for LPL vs. mean fluorescence intensity = 26,183 for MLNs). Surprisingly, although BTLA is an inhibitory receptor, *Btla*$^{-/-}$ T cells transferred into *Rag*$^{-/-}$ animals induced colitis similar to WT donors when weight loss was measured (Fig. 6 C). Histological analysis performed 2 wk after transfer revealed higher average scores for recipients transferred with *Btla*$^{-/-}$ T cells, but there was no difference at 5 wk (Fig. 6 D).

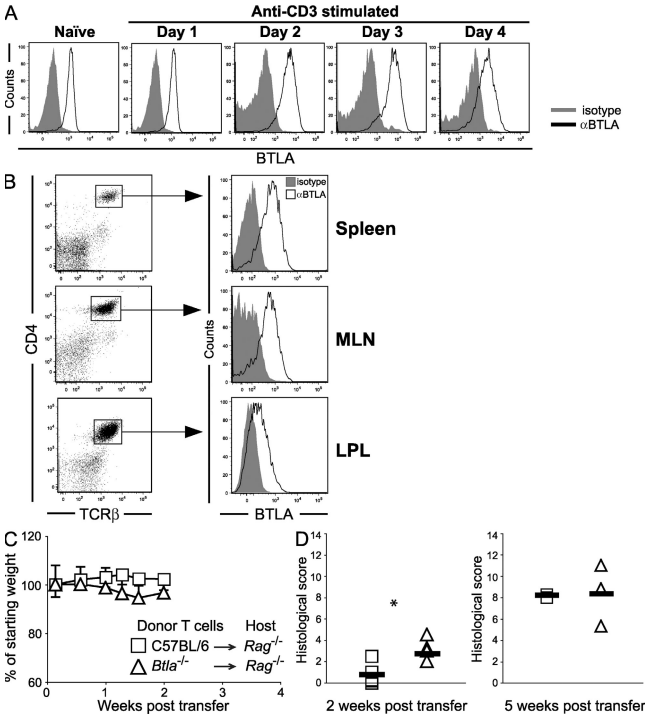

Figure 6. Minimal effect of T cell BTLA deficiency on colitis pathogenesis. (A) BTLA expression on freshly isolated naive CD4$^+$ T cells and by CD4$^+$ T cells stimulated in vitro with an anti-CD3ε mAb in the presence of irradiated T cell–depleted splenocytes. (B) BTLA expression on transferred CD4$^+$ T cells isolated from *Hvem*$^{-/-}$*Rag*$^{-/-}$ recipients 2 wk after transfer. Histograms represent BTLA expression by gated CD4$^+$ TCR-β$^+$ cells from the indicated sites. (C) Transfer of *Btla*$^{-/-}$ CD4$^+$CD45RB^{high} T cells into *Rag*$^{-/-}$ recipients. Weight loss curves of *Rag*$^{-/-}$ recipients transferred with either WT T cells (squares) or *Btla*$^{-/-}$ T cells (triangles). Data shown represent the average of six to eight mice in each group. (D) Histological scores were evaluated 2 (left) or 5 wk (right) after the transfer of T cells. Each symbol represents an individual mouse (n = 5–8). Data are representative of four independent experiments. *, $P < 0.05$.

Reduced number of BTLA-deficient T cells in *Rag*$^{-/-}$ recipients

It has been recently shown that BTLA plays a role in the survival of T cells activated in a mouse GVHD model (32). In light of our finding that *Rag*$^{-/-}$ recipients of BTLA-deficient T cells did not develop accelerated colitis, we hypothesized that BTLA-deficient T cells transferred into *Rag*$^{-/-}$ recipients might have a survival defect, leading to a reduced number of effector T cells that ultimately might affect the onset of colitis. To address this possibility, we performed cotransfers of equal numbers of WT CD45.1$^+$ congenic and *Btla*$^{-/-}$ CD45.2$^+$ CD4$^+$CD45RB^{high} T cells into *Rag*$^{-/-}$ recipients. *Btla*$^{-/-}$ T cells did not accumulate as much as WT cells. The percentages (Fig. 7 A) and absolute numbers (Fig. 7 B) of CD45.1$^+$ CD4$^+$ TCR-β$^+$ cells in the spleens, MLNs, LPLs, and intestinal epithelial lymphocytes (IELs) were considerably higher than those for *Btla*$^{-/-}$ (CD45.1$^-$) T cells 2 wk after transfer. Although the *Btla*$^{-/-}$ T cells did not accumulate as much as WT donors, the BTLA-deficient T cells in *Rag*$^{-/-}$ mice were capable of secreting proinflammatory cytokines to a similar extent (Fig. 7 C). Based on these findings, we hypothesize that transfer of *Btla*$^{-/-}$ T cells did not recapitulate the results in *Hvem*$^{-/-}$*Rag*$^{-/-}$ recipients in part because the lower numbers of effector T cells prevented disease acceleration.

Signaling through BTLA prevented colitis acceleration

To further explore the role of the BTLA inhibitory receptor, we evaluated colitis development in recipient *Hvem*$^{-/-}$ *Rag*$^{-/-}$ mice treated with an anti-BTLA mAb (clone 6F7). When added to T cell–APC co-cultures stimulated with an anti-CD3ε antibody, the 6F7 antibody attenuated T cell responses. The expression of CD25 and the production of IL-2 by anti-BTLA–treated T cells were reduced compared with the IgG-treated control (Fig. S4, available at http://www.jem.org/cgi/content/full/jem.20071160/DC1). Importantly, the inhibitory effect on immune responses mediated by the 6F7 antibody was specific to BTLA-expressing T cells, as the activation and proliferation of *Btla*$^{-/-}$ T cells was essentially equivalent in cultures treated with the 6F7 mAb or an irrelevant IgG control (Fig. S4 B). The anti-BTLA mAb reduced IL-2 and CD25 induction even when *Hvem*$^{-/-}$ T cells and APCs were co-cultured (Fig. S4 D), indicating that the mAb acts directly by engaging BTLA, as opposed to blocking interactions with HVEM. These results indicate that the anti-BTLA mAb 6F7 has agonistic activity that stimulates BTLA-mediated inhibitory signals leading to decreased T cell–immune responses in vitro.

We found that the anti-BTLA mAb also has agonistic activity in vivo. Injection of the anti-BTLA mAb every 3 d beginning at the time of T cell transfer greatly delayed weight loss and disease progression (Fig. 8 A). Furthermore, *Hvem*$^{-/-}$*Rag*$^{-/-}$ recipients treated with the anti-BTLA mAb had lower average histological scores (Fig. 8 B). Collectively, these results demonstrate that BTLA engagement was required to prevent colitis acceleration, and they suggest that the rapid development of disease in *Hvem*$^{-/-}$*Rag*$^{-/-}$ mice is likely to be caused by the absence of BTLA signaling.

To evaluate if the anti-BTLA mAb prevents colitis by acting on donor T cells, we transferred *Btla*$^{-/-}$ CD4$^+$CD45RB^{high} T cells into *Hvem*$^{-/-}$*Rag*$^{-/-}$ recipients that were then treated with the anti-BTLA mAb. *Hvem*$^{-/-}$*Rag*$^{-/-}$ mice transferred with *Btla*$^{-/-}$ T cells showed faster weight loss regardless of treatment with the anti-BTLA mAb (Fig. 8 C). In addition, all the transferred animals presented with severe intestinal inflammation and similar histological average scores (Fig. 8 D). These results demonstrate that the anti-BTLA mAb prevents colitis acceleration when the donor T cells express BTLA. Therefore, we conclude that BTLA signaling on T cells mediated by HVEM expressed by an irradiation-resistant cell is crucial to prevent colitis acceleration.

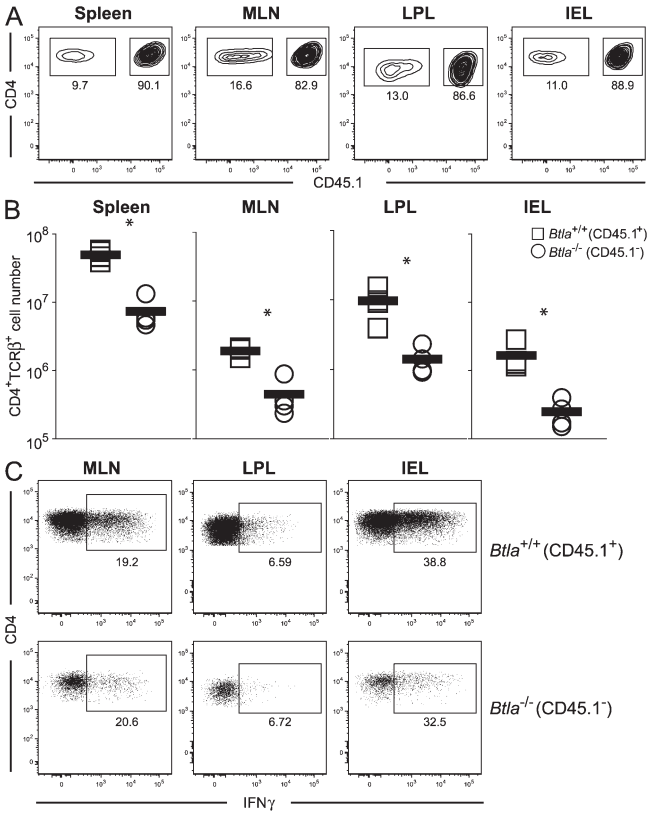

Figure 7. Reduced accumulation of *Btla*$^{-/-}$ T cells in *Rag*$^{-/-}$ recipients. Co-transfer of congenic CD45.1$^+$ and CD45.2$^+$ *Btla*$^{-/-}$ CD4$^+$CD45RB^{high} T cells into *Rag*$^{-/-}$ recipients. (A) Representative percentages of CD45.1$^+$ (*Btla*$^{+/+}$) and CD45.1$^-$ (*Btla*$^{-/-}$) CD4$^+$ TCR-β$^+$ cells in the spleens, MLNs, LPLs, and IELs of *Rag*$^{-/-}$ mice analyzed 2 wk after T cell transfer. (B) Same as A, but showing absolute numbers of CD45.1$^+$ (squares) and CD45.1$^-$ (circles) CD4$^+$TCR-β$^+$ T cells. Each symbol represents an individual mouse ($n = 4$). *, $P < 0.05$. (C) Intracellular IFN-γ staining of CD4$^+$TCR-β$^+$ CD45.1$^+$ (top dot plots) and CD45.1$^-$ (bottom dot plots) T cells isolated from *Rag*$^{-/-}$ mice and restimulated ex vivo with PMA and ionomycin. Data shown correspond to a single mouse in a total of four mice per group and are representative of two independent experiments.

Accelerated colitis in *Btla*$^{-/-}$*Rag*$^{-/-}$ recipients

Although the effect of the agonistic anti-BTLA mAb required BTLA expression by T cells, the experiments presented above prove only that T cell expression of BTLA is necessary, but not sufficient, and therefore it remained possible that BTLA expression by host cells in the *Rag*$^{-/-}$ mice may also be required for preventing colitis acceleration. To investigate this possibility, we used *Btla*$^{-/-}$*Rag*$^{-/-}$ animals as recipients of WT CD4$^+$CD45RB^{high} T cells. The transfer of T cells into *Btla*$^{-/-}$*Rag*$^{-/-}$ recipients led to faster weight loss (Fig. 9 A). Furthermore, histological analysis performed 2 wk after the transfer on samples isolated from the large intestine revealed a more severe intestinal inflammation in *Btla*$^{-/-}$*Rag*$^{-/-}$ mice (Fig. 9 B). To determine if disease acceleration in *Btla*$^{-/-}$*Rag*$^{-/-}$ mice was comparable to that observed in HVEM-deficient

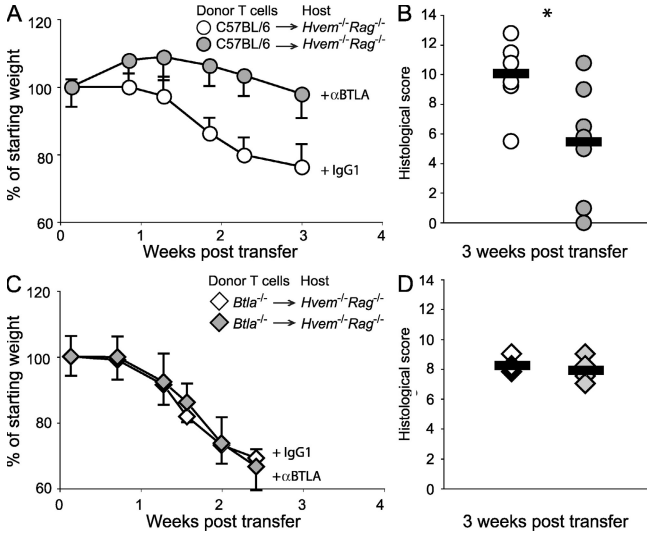

Figure 8. Signaling through BTLA prevents colitis acceleration in *Hvem*$^{-/-}$*Rag*$^{-/-}$ recipients. (A) Weight loss curves of *Hvem*$^{-/-}$*Rag*$^{-/-}$ mouse recipients of WT T cells treated with either 100 µg anti-BTLA mAb (clone 6F7) or IgG1 isotype control twice a week beginning at the time of T cell transfer. Data shown represent the average of four mice in each group and are representative of two independent experiments. (B) Histological scoring performed 3 wk after T cell transfer revealed milder intestinal inflammation in samples obtained from *Hvem*$^{-/-}$*Rag*$^{-/-}$ animals treated with the anti-BTLA mAb. Each circle represents a single mouse in a total of eight mice per group. *, $P < 0.05$. (C) Same as A, except that *Hvem*$^{-/-}$*Rag*$^{-/-}$ animals were transferred with *Btla*$^{-/-}$ CD4$^+$CD45RB^{high} T cells. (D) Histological analysis 3 wk after transfer revealed equivalent intestinal inflammation in all transferred *Hvem*$^{-/-}$*Rag*$^{-/-}$ animals regardless of the treatment with the anti-BTLA mAb. Each circle represents a single mouse in a total of five mice per group.

hosts, WT CD4$^+$CD45RB^{high} were simultaneously transferred into *Btla*$^{-/-}$*Rag*$^{-/-}$ or *Hvem*$^{-/-}$*Rag*$^{-/-}$ mice. In the two groups of recipients, colitis development was essentially equivalent. Although the trend was toward slightly less weight loss and less severe histological scores in *Btla*$^{-/-}$*Rag*$^{-/-}$ mice than in *Hvem*$^{-/-}$*Rag*$^{-/-}$ mice, the difference did not reach statistical significance (Fig. 9, C and D). Similar results were obtained when *Btla*$^{-/-}$*Rag*$^{-/-}$ recipients were transferred with *Btla*$^{-/-}$ CD4$^+$CD45RB^{high}, a situation where BTLA was absent in both donor and host cells (Fig. 9, C and D). Collectively, these results demonstrate that BTLA expression by *Rag*$^{-/-}$ host cells also prevents accelerated colitis in the T cell transfer model.

DISCUSSION

HVEM is a unique TNF family receptor because it has the ability both to transmit positive signals and to induce negative signals. Subsets of T cells constitutively express HVEM, and therefore it is perhaps not surprising that many of the experiments analyzing the role of HVEM have focused on T lymphocytes. HVEM expressed by T cells is a co-stimulatory receptor for LIGHT-mediated T cell activation (8, 9, 18, 22, 25). Furthermore, recent reports demonstrated that HVEM also engages BTLA and inhibits T cell proliferation (25, 26, 43).

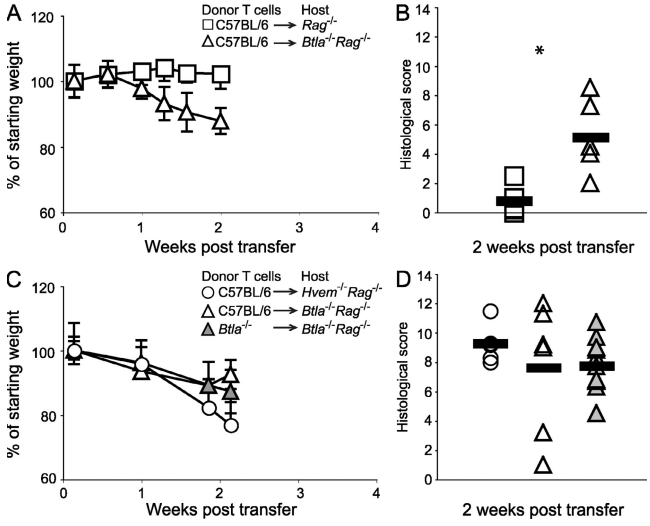

Figure 9. Accelerated colitis in *Btla*$^{-/-}$*Rag*$^{-/-}$ recipients. (A) Weight loss curves of *Rag*$^{-/-}$ (squares) and *Btla*$^{-/-}$*Rag*$^{-/-}$ (triangles) recipients transferred with 5 × 10^5 WT T cells. Data correspond to the average of four to six mice per group. (B) Combined proximal and distal colon histological scores were evaluated 2 wk after T cell transfer. Each symbol represents an individual mouse from a total of six to seven animals per group. (C) Weight loss curves of *Hvem*$^{-/-}$*Rag*$^{-/-}$ (circles) and *Btla*$^{-/-}$*Rag*$^{-/-}$ (open triangles) recipients transferred with 5 × 10^5 WT T cells, and *Btla*$^{-/-}$*Rag*$^{-/-}$ mice transferred with 5 × 10^5 *Btla*$^{-/-}$ T cells (filled triangles). Data correspond to the average of four to six mice per group and are representative of two independent experiments. (D) Histological scores performed on samples obtained from two independent experiments 2 wk after T cell transfer. Each symbol represents an individual mouse from a total of 5–11 animals per group. *, $P < 0.05$.

Hvem$^{-/-}$ mice do not have a dramatic phenotype, however, which might reflect the balance between the activating and inhibitory signals mediated by HVEM.

In this report, we analyzed the role of HVEM in intestinal inflammation induced by the transfer of naive CD4$^+$ T cells into *Rag*$^{-/-}$ mice. This experimental system is well suited to the analysis of complex networks of receptor–ligand interactions because disease development is synchronous and the genotypes of the donor T cells and the immune-deficient host can be independently varied. The most striking finding in the work presented here was the dramatic acceleration of colitis observed in *Hvem*$^{-/-}$*Rag*$^{-/-}$ mice transferred with WT CD4$^+$CD45RB^{high} T cells. Clinical signs correlated with an extremely fast weight loss and elevated histological scores in the colon within 2 wk after T cell transfer. Colitis acceleration in *Hvem*$^{-/-}$*Rag*$^{-/-}$ recipient mice was characterized by a rapid accumulation of activated T cells producing Th1 cytokines and IL-17 in the large intestine of these recipients. This suggests that colitis acceleration is probably induced by an exacerbated proinflammatory response mediated by CD4$^+$ T cells in the large intestine.

Because of the surprising acceleration of disease in *Hvem*$^{-/-}$*Rag*$^{-/-}$ mice, we performed experiments to identify the critical cell type(s) that must express HVEM. Although APCs were considered the most promising candidate, we could find little evidence for a global alteration in APC function in *Hvem*$^{-/-}$ mice, although T cells cultured in vitro with *Hvem*$^{-/-}$ MLN DCs and a soluble anti-CD3ε mAb did exhibit a slightly enhanced proliferative response. Surprisingly, transfer experiments using BM chimeric mice revealed that HVEM expression on a radioresistant cell population in the *Rag*$^{-/-}$ animals is most critical for preventing colitis acceleration. Moreover, we found that mouse IECs expressed high levels of HVEM. IECs are a main point of contact for enteric antigens, and they play a direct role in regulating T cell responses to these antigens (44). It has been recently shown that IECs may contribute to the maintenance of T cell tolerance in the gut by preventing inappropriate activation of CD4$^+$ T cells (45, 46), and they express PD-L1, the ligand for the inhibitory receptor programmed cell death 1 (46). Nevertheless, although epithelial cell expression of HVEM is intriguing, IEC permeability was not altered in *Hvem*$^{-/-}$ mice, and these mice were not more susceptible to DSS colitis. Therefore, the absence of HVEM does not alter IEC physiological function in the absence of T cell–induced inflammation, and it remains to be proven that HVEM expression by IECs is required to prevent colitis acceleration. A radioresistant, tissue-specific APC expressing CD70, and required for the proliferation of mucosal T cells after oral infection, was recently identified (47), and therefore these cells or some other radioresistant HVEM-expressing cell type could be most responsible for preventing accelerated colitis. Conditional ablation of HVEM expression in different cell types in *Rag*$^{-/-}$ mice with a floxed *Hvem* allele ultimately will be required to identify the cell type(s) that must express this protein to prevent disease acceleration.

Although HVEM is expressed by the transferred T cells (not depicted), the absence of HVEM in the donor T lymphocytes slightly reduced the severity of colitis development. Therefore, HVEM expression by T cells apparently contributed to the enhancement of T cell effector function, opposite to the effect of HVEM expression by cells in the RAG-deficient hosts. By binding to the TNF family ligand LIGHT, HVEM mediates co-stimulatory signals (11, 12, 19, 23, 24), and it was recently shown that the severity of colitis induced by the transfer of LIGHT-transgenic MLN cells into $Rag^{-/-}$ recipients was considerably decreased when the MLN cells were obtained from $Hvem^{-/-}$ mice (6). The authors concluded that HVEM expression on T cells is necessary for optimal LIGHT-mediated T cell activation and expansion in this system (6). Therefore, T cell–derived LIGHT interacting with HVEM expressed by the same or an adjacent T cell may be required for the full Th1 and/or Th17 differentiation of gut-homing effector T cells (4). Evidence suggesting a potential for T–T interactions between LIGHT and HVEM on donor T cells also has been developed in a GVHD model system (48). Consistent with the co-stimulatory role of LIGHT, we found that mice transferred with $Light^{-/-}$ $CD4^+CD45RB^{high}$ T cells also had lower histological scores. It is noteworthy that if the effect of HVEM deficiency in the RAG-deficient host were mediated predominantly by interactions with T cell–expressed LIGHT, colitis should have been accelerated, rather than delayed, after transfer of $Light^{-/-}$ $CD4^+CD45RB^{high}$ T cells. When either $Light^{-/-}$ or $Hvem^{-/-}$ $CD4^+CD45RB^{high}$ T cells were transferred into $Hvem^{-/-}Rag^{-/-}$ animals, however, the disease-accelerating effects of the absence of HVEM in the $Rag^{-/-}$ host were dominant over the more subtle disease-delaying effects when these molecules were not expressed by the gene-deficient donor T cells. Therefore, the predominant effect of HVEM in this colitis model system is antiinflammatory, and it is related to its expression by radiation-resistant innate cells in the $Rag^{-/-}$ hosts.

Because BTLA is an inhibitory receptor for T cells, it was a good candidate for mediating the antiinflammatory effect of HVEM expression in the $Rag^{-/-}$ recipients. Consistent with this hypothesis, treatment of $Hvem^{-/-}Rag^{-/-}$ recipients of $CD4^+CD45RB^{high}$ T cells with an anti-BTLA mAb with agonistic properties was able to reverse the accelerated colitis, but only when the T cells expressed BTLA. Although our data clearly demonstrate that a major function of the anti-BTLA mAb is to attenuate T cell responses, BTLA expression by host cells is also relevant. The transfer of WT T cells into BTLA-deficient $Rag^{-/-}$ recipients also led to accelerated colitis, indicating that T cell expression of BTLA is necessary but not sufficient, and that there also is a function for BTLA expression by host cells in preventing colitis acceleration. BTLA expression has been detected on myeloid and lymphoid cells, including $CD11c^+$ DCs, a subpopulation of $CD11b^+$ macrophages and also $DX5^+$ NK cells (27, 42). Interestingly, NK cells have been shown to prevent accelerated colitis development in the T cell transfer model of colitis (49). Therefore, engagement of BTLA on one or more of these innate immune cell types could contribute to moderating colitis progression.

During the review of this paper, it was shown in human cells that HVEM binds to CD160, a glycophosphatidylinositol-anchored member of the Ig super family (50). The authors of this report found that the binding of CD160 by HVEM delivered inhibitory signals to human $CD4^+$ T cells, leading to reduced T cell activation and cytokine production (50). Although it is not known if this interaction takes place in mice, we cannot rule out the possibility of an antiinflammatory role for the HVEM–CD160 interaction in the experimental colitis model. Consistent with a possible role for CD160, when $Btla^{-/-}Rag^{-/-}$ mice were transferred with $CD4^+$ T cells, weight loss and histological scores were less severe than in $Hvem^{-/-}Rag^{-/-}$ recipients. Although the differences were not statistically significant, the trend was toward milder disease in $Btla^{-/-}Rag^{-/-}$ mice. This was also observed when $Btla^{-/-}Rag^{-/-}$ mice were transferred with BTLA-deficient T cells, a situation where the HVEM–BTLA interaction is completely ablated. The difference in colitis between HVEM and BTLA deficiency is not very great, however, suggesting that most of the disease-accelerating effects of HVEM deficiency are due to interaction with BTLA as opposed to the absence of a hypothetical interaction of mouse HVEM with CD160.

Contrary to our expectations, the transfer of $Btla^{-/-}$ $CD4^+CD45RB^{high}$ T cells into $Rag^{-/-}$ mice did not replicate the severe disease phenotype in the $Hvem^{-/-}Rag^{-/-}$ recipients. Surprisingly, we found that there was a significant reduction in the number of T cells in different lymphoid organs and in the large intestine after transfer of $Btla^{-/-}$ $CD4^+$ T cells. In accordance with this finding, it has recently been shown that under conditions of chronic stimulation in a GVHD model system, $Btla^{-/-}$ T cells did not survive as well and failed to sustain GVHD pathology (32). Therefore, decreased T cell survival could partially explain the absence of a dramatic colitis acceleration after transfer of $Btla^{-/-}$ T cells into $Rag^{-/-}$ mice. It should be noted that after transfer of $Btla^{-/-}$ T cells into $Rag^{-/-}$ mice, HVEM can still induce inhibitory signals by interacting with BTLA expressed by host cells. However, when the stromal cells cannot deliver the critical antiinflammatory HVEM-mediated signals to either the transferred T cells or to $Rag^{-/-}$ host cells, as is the case in $Hvem^{-/-}Rag^{-/-}$ recipients, accelerated disease occurs, even after transfer of $Btla^{-/-}$ $CD4^+$ T cells.

In summary, HVEM can act as a receptor to enhance immune responses through binding LIGHT and as a ligand to suppress immune response by binding BTLA. It is therefore not surprising that HVEM plays a dual role in the development of colitis. By analyzing *Hvem*-deficient mice and cells, previous studies and the work presented here indicate that the lack of HVEM expression by T cells decreased T cell activation and the development of effector functions. The effects of HVEM deficiency are cell type dependent; however, the lack of HVEM expression by an irradiation-resistant cell type(s) in the immune-deficient recipients caused an acceleration of intestinal inflammation. $Hvem^{-/-}$ mice do not spontaneously develop colitis, however, and it is likely that in immune-competent mice $CD4^+CD25^+$ regulatory T cells or

other mechanisms prevent gut inflammation. Moreover, the counterbalancing effects of HVEM expression by different cell types, and the dual engagement of proinflammatory LIGHT and antiinflammatory BTLA by HVEM, may explain the absence of spontaneous colitis in *Hvem*$^{-/-}$ mice. Our findings therefore depended critically on the power of the T cell transfer model of colitis in analyzing cell–cell interactions and the interplay of the innate adaptive immune systems, as we could separate the proinflammatory and antiinflammatory effects of HVEM expression by comparing *Hvem*$^{-/-}$ T cell donors and *Hvem*$^{-/-}$*Rag*$^{-/-}$ recipients to their WT counterparts. Although the majority of studies on HVEM have addressed the participation of this molecule when expressed by T cells or APCs, our studies demonstrate the unexpected and important role that this molecule plays to prevent inflammation when expressed by irradiation-resistant nonlymphoid cells. The expression of HVEM and BTLA on both innate and adaptive cells, along with the findings presented here, suggest that this ligand–receptor system could play diverse roles in immunity and inflammation in both the innate and adaptive immune systems that have yet to be fully elucidated.

MATERIALS AND METHODS

Mice. C57BL/6, *Rag*$^{-/-}$ (C57BL/6 background), and C57BL/6-SJL CD45.1 congenic mice were purchased from The Jackson Laboratory and maintained in our facility. *Btla*$^{-/-}$ (28), *Light*$^{-/-}$ (37), and *Hvem*$^{-/-}$ mice (26) have been described previously. All gene-deficient mice were backcrossed for at least six generations onto the C57BL/6 background. *Hvem*$^{-/-}$ or *Btla*$^{-/-}$ mice were crossed to *Rag*$^{-/-}$ mice to generate *Hvem*$^{-/-}$*Rag*$^{-/-}$ and *Btla*$^{-/-}$*Rag*$^{-/-}$ recipient animals, respectively. Mice were maintained at the La Jolla Institute for Allergy and Immunology under specific pathogen-free conditions, and sentinels from the mouse colony tested negative by PCR detection of *Helicobacter spp*. and *Citrobacter rodentium*. Mice were used at 7–12 wk of age. Animal care and experimentation were consistent with the National Institutes of Health guidelines and were approved by the Institutional Animal Care and Use Committee at the La Jolla Institute for Allergy and Immunology.

Antibodies and reagents. The following mouse antibodies were purchased from BD Biosciences as conjugated to FITC, PE, PE-Cy5, PerCP-Cy5.5, or allophycocyanin: CD4 (L3T4), CD45RB (16A), CD45.2 (104), TCR β chain (H57-597), and rat anti–hamster IgG (cocktail). A PE-conjugated and purified anti–mouse BTLA mAb (6F7) were purchased from eBioscience and Bio Express, Inc., respectively. Anti–mouse HVEM antibody (26) was provided by Y.X. Fu (University of Chicago, Chicago, IL). Anti–mouse CD16/32 used for Fc receptor blocking was purified in our laboratory. Purified mouse IgG1 was purchased from Millipore.

CD4$^+$ CD45RB^{high} T cell isolation and transfers. Spleens were removed from the donor mice (C57BL/6, *Light*$^{-/-}$, *Hvem*$^{-/-}$, *Btla*$^{-/-}$, or B6-SJL CD45 congenic) and teased into cell-single suspensions in HBSS media (Invitrogen). Cell suspensions were filtered through a 70-μm cell strainer (Thermo Fisher Scientific), and then CD4$^+$ cells were enriched by positive selection using anti-CD4 (L3T4) microbeads according to the manufacturer's protocol (Miltenyi Biotec). The CD4$^+$-enriched cells were washed twice and stained with PE-Cy5–conjugated anti-CD4 and PE-conjugated anti-CD45RB antibodies. After staining, the cells were washed, and the CD4$^+$CD45RB^{high} T cell population was sorted by flow cytometry using a FACS-DIVA cell sorter (Becton Dickinson). Purified CD4$^+$CD45RB^{high} naive T cells were washed twice and resuspended in PBS, and 5×10^5 cells in 200 μl of PBS were injected i.v. into the different recipient mice. Transferred mice were monitored regularly for signs of disease, including weight loss, hunched over appearance, piloerection of the coat, and diarrhea. For cotransfer experiments, CD4$^+$CD45RB^{high} T cells were isolated from congenic CD45.1$^+$ and CD45.2$^+$ *Btla*$^{-/-}$ mice, mixed in equal numbers and injected i.v. into *Rag*$^{-/-}$ recipients.

Preparation of IELs and LPLs. Mucosal lymphocytes were isolated and prepared as described previously (34). In brief, the large intestine was removed and placed in chilled HBSS media containing 5% FCS. The intestines were carefully cleaned from their mesenteries and flushed of fecal content. Intestines were opened longitudinally and cut into 1-cm pieces. The intestinal tissue was transferred to 250-ml Erlenmeyer flasks containing 25 ml of preheated HBSS supplemented with 2% FBS and 1 mM DTT (Sigma-Aldrich) and shaken at 200 rpm for 40 min at 37°C. The tissue suspensions were passed through a stainless steal sieve into 50-ml conical tubes, and the cells were pelleted by centrifugation at 1,200 rpm for 10 min at 4°C. The cell pellets were resuspended in complete HBSS, layered over a discontinuous 40/70% Percoll (GE Healthcare) gradient, and centrifuged at 2,000 rpm for 30 min. Cells from the 40/70% interface were collected, washed, and resuspended in complete RPMI media (Invitrogen). These purified cells constituted the IEL population. To isolate LPLs, the remaining intestinal tissue in the stainless steal sieve was minced and transferred to conical tubes. The minced pieces were resuspended in 20 ml of complete RPMI containing 1 mg/ml of type IV collagenase (Sigma-Aldrich) and shaken at 200 rpm for 40 min at 37°C. The tissue suspension was collected and passed through a 70-μm cell strainer, and then the cells were pelleted by centrifugation at 1,200 rpm. The cells were then resuspended and layered onto a 40/70% Percoll gradient, centrifuged, and processed as described above for the IEL preparation.

Histology. At various time points after cell transfer, animals were killed for histological analysis. Tissue samples of 3–5 mm obtained from distal and proximal portions of the large intestine were fixed in 4% formalin. Fixed tissues were later embedded in paraffin and 3-μm sections were prepared and stained with H&E. To evaluate the severity of the inflammation, samples were coded and scored by a pathologist in a blinded fashion using a previously described scoring system (34). Scores from the two parts of the intestine were averaged to represent the severity of disease. Higher scores (maximum 14) indicate greater pathology. Categories scored are the following: degree of inflammatory cell infiltrate in the lamina propria, goblet cell depletion, epithelial cell reactive atypia/hyperplasia, number of IELs in epithelial crypts, and number of inflammatory foci.

Flow cytometry analysis. Spleens and MLNs were removed and then mashed through a 70-μm cell strainer, and red blood cells in the cell suspension were removed using a lysing buffer (Sigma-Aldrich). IELs and LPLs were isolated as described above. Before staining, cells were washed and resuspended in staining buffer containing 1× PBS, 2% BSA, 10 mM EDTA, and 0.01 NaN_3. To block nonspecific staining, anti-CD16/32 antibody was added. Antibodies for cell surface markers were added, and cells were incubated for 20 min on ice. After staining, the cells were washed twice with staining buffer, analyzed the same day or fixed in PBS containing 1% paraformaldehyde and 0.01 NaN_3, and analyzed later in a FACSCalibur (BD Biosciences).

Detection of cytokines by ELISA. 2 wk after the transfer of CD4$^+$CD45RB^{high} T cells, LPLs were isolated from the recipients and 10^6 cells were cultured in RPMI complete medium in the presence of PMA and ionomycin for 48 h. The amounts of IFN-γ, IL-4, TNF, and IL-2 in the culture supernatants were quantified by ELISA. Antibodies and recombinant cytokine standards were purchased from BD Biosciences.

RNA isolation and real-time PCR. 2 wk after the transfer of CD4$^+$CD45RB^{high} T cells, 1.5 cm from the large intestines of the recipients was removed and resuspended in TRIZol (Invitrogen). The samples were

then frozen at −80°C. For RNA isolation, the whole tissue was homogenized, DNA and proteins were removed by precipitation with chloroform, and RNA was extracted with isopropanol. cDNA was synthesized from the total RNA using the Superscript II system (Invitrogen) according to the manufacturer's instructions. Subsequently, the cDNA was subject to real-time PCR using SYBR green (Bio-Rad Laboratories) and the following mouse primers: TNF forward, 5′-CATCTTCTCAAAATTCGAGTGACAA-3′; TNF reverse, 5′-TGGGAGTAGACAAGGTACAACCC-3′; IFN-γ forward, 5′-TCAAGTGGCATAGATGTGGAAGAA-3′; IFN-γ reverse, 5′-TGGCTCTGCAGGATTTTCATG-3′; IL-4 forward, 5′-ACAGGAGAAGGGACGCCAT-3′; IL-4 reverse, 5′-GAAGCCCTACAGACGAGCTCA-3′; IL-17 forward, 5′-GGTCAACCTCAAAGTCTTTAACTC-3′; IL-17 reverse, 5′-TTAAAAATGCAAGTAAGTTTGCTG-3′; IL-12p35 forward, 5′-TGAAGACGGCCAGAGAAAAAC-3′; IL-12p35 reverse, 5′-AAGGAACCCTTAGAGTGCTTACT-3′; IL-23p19 forward, 5′-AGCGGGACATATGAATCTACTAAGAGA-3′; IL-23p19 reverse, 5′-GTCCTAGTAGGGAGGTGTGAAGTTG-3′; IL-10 forward, 5′-GGTTGCCAAGCCTTATCGGA-3′; IL-10 reverse, 5′-ACCTGCTCCACTGCCTTGCT-3′; TGF-β forward, 5′-TGACGTCACTGGAGTTGTACGG-3′; TGF-β reverse, 5′-GGTTCATGTCATGGATGGTGC-3′; L32 forward, 5′-GAAACTGGCGGAAACCCA-3′; and L32 reverse, 5′-GGATCTGGCCCTTGAACCTT-3′. Gene expression was normalized to L32. Data were collected and analyzed on an iCycler (Bio-Rad Laboratories).

Generation of BM chimeras. $Rag^{-/-}$ or $Hvem^{-/-}Rag^{-/-}$ hosts were lethally irradiated with 11 Gy that were applied in two irradiations of 5.5 Gy separated by a 3-h interval. After irradiation, $Hvem^{-/-}Rag^{-/-}$ hosts were transplanted with 5×10^6 total BM cells isolated from $Rag^{-/-}$ mice to generate $Rag^{-/-}\rightarrow Hvem^{-/-}Rag^{-/-}$ chimeric animals. Reciprocal $Hvem^{-/-}Rag^{-/-}\rightarrow Rag^{-/-}$ chimeras were generated by transplanting $Hvem^{-/-}Rag^{-/-}$ BM cells into irradiated $Rag^{-/-}$ hosts. After transplant, mice were maintained under antibiotic treatment for 4 wk and an additional 6 wk without antibiotic before transfer of the $CD4^+CD45RB^{high}$ T cells.

Statistics. Differences between groups were evaluated for statistical significance by the two-tailed unpaired Student's *t* test, except for histological scoring that was evaluated using Wilcoxon's two-group test. Results are expressed as mean ± SD. p-values of <0.05 were considered significant.

Online supplemental material. Fig. S1 (A and B) shows, respectively, the phenotype of freshly isolated or LPS-stimulated $CD11c^+$ cells isolated from the MLNs of WT or $Hvem^{-/-}$ mice. Fig. S1 C shows proliferation assessed by CFSE dilution of $CD4^+CD25^-$ T cells cultured with WT or $Hvem^{-/-}$ $CD11c^+$ and an anti-CD3ε mAb. Fig. S2 A shows HVEM expression on purified primary colonic epithelial cells. Fig. S2 B shows the results from intestinal permeability experiments performed on distal colons isolated from untreated WT and $Hvem^{-/-}$ mice or WT animals treated with 4% DSS. Fig. S3 (A and B) shows, respectively, weight loss curves and histological scores of WT and $Hvem^{-/-}$ mice treated with 2.5% DSS. Fig. S4 (A–D) shows the effect of an anti-BTLA mAb (6F7) on T cell activation, in particular CD25 expression and IL-2 production. The online supplemental material is available at http://www.jem.org/cgi/content/full/jem.20071160/DC1.

We would like to thank Christopher Lena for technical assistance, and Hilde Cheroutre, Daniel Mucida, and Marta Lopez-Fraga for critical comments and advice.

This work was supported by grants from the National Institutes of Health AI61516 (to M. Kronenberg) and AI33068 (to C.F. Ware), by a Research Fellowship Award from the Crohn's & Colitis Foundation of America (to M.W. Steinberg), and by the University of California, San Diego, Digestive Diseases Research Development Center (DK 080506). This is manuscript number 850 from the La Jolla Institute for Allergy and Immunology.

The authors have no conflicting financial interests.

Submitted: 7 June 2007
Accepted: 15 May 2008

REFERENCES

1. Bouma, G., and W. Strober. 2003. The immunological and genetic basis of inflammatory bowel disease. *Nat. Rev. Immunol.* 3:521–533.
2. Sartor, R.B. 2003. Innate immunity in the pathogenesis and therapy of IBD. *J. Gastroenterol.* 38:43–47.
3. Targan, S.R. 2000. Biology of inflammation in Crohn's disease: mechanisms of action of anti-TNF-a therapy. *Can. J. Gastroenterol.* 14:13C–16C.
4. Cohavy, O., J. Zhou, S.W. Granger, C.F. Ware, and S.R. Targan. 2004. LIGHT expression by mucosal T cells may regulate IFN-gamma expression in the intestine. *J. Immunol.* 173:251–258.
5. Cohavy, O., J. Zhou, C.F. Ware, and S.R. Targan. 2005. LIGHT is constitutively expressed on T and NK cells in the human gut and can be induced by CD2-mediated signaling. *J. Immunol.* 174:646–653.
6. Wang, J., R.A. Anders, Y. Wang, J.R. Turner, C. Abraham, K. Pfeffer, and Y.X. Fu. 2005. The critical role of LIGHT in promoting intestinal inflammation and Crohn's disease. *J. Immunol.* 174:8173–8182.
7. Gommerman, J.L., and J.L. Browning. 2003. Lymphotoxin/light, lymphoid microenvironments and autoimmune disease. *Nat. Rev. Immunol.* 3:642–655.
8. Tamada, K., K. Shimozaki, A.I. Chapoval, Y. Zhai, J. Su, S.F. Chen, S.L. Hsieh, S. Nagata, J. Ni, and L. Chen. 2000. LIGHT, a TNF-like molecule, costimulates T cell proliferation and is required for dendritic cell-mediated allogeneic T cell response. *J. Immunol.* 164:4105–4110.
9. Tamada, K., K. Shimozaki, A.I. Chapoval, G. Zhu, G. Sica, D. Flies, T. Boone, H. Hsu, Y.X. Fu, S. Nagata, et al. 2000. Modulation of T-cell-mediated immunity in tumor and graft-versus-host disease models through the LIGHT co-stimulatory pathway. *Nat. Med.* 6:283–289.
10. Wan, X., J. Zhang, H. Luo, G. Shi, E. Kapnik, S. Kim, P. Kanakaraj, and J. Wu. 2002. A TNF family member LIGHT transduces costimulatory signals into human T cells. *J. Immunol.* 169:6813–6821.
11. Shaikh, R.B., S. Santee, S.W. Granger, K. Butrovich, T. Cheung, M. Kronenberg, H. Cheroutre, and C.F. Ware. 2001. Constitutive expression of LIGHT on T cells leads to lymphocyte activation, inflammation, and tissue destruction. *J. Immunol.* 167:6330–6337.
12. Wang, J., J.C. Lo, A. Foster, P. Yu, H.M. Chen, Y. Wang, K. Tamada, L. Chen, and Y.X. Fu. 2001. The regulation of T cell homeostasis and autoimmunity by T cell-derived LIGHT. *J. Clin. Invest.* 108:1771–1780.
13. Anders, R.A., S.K. Subudhi, J. Wang, K. Pfeffer, and Y.X. Fu. 2005. Contribution of the lymphotoxin beta receptor to liver regeneration. *J. Immunol.* 175:1295–1300.
14. Endres, R., M.B. Alimzhanov, T. Plitz, A. Futterer, M.H. Kosco-Vilbois, S.A. Nedospasov, K. Rajewsky, and K. Pfeffer. 1999. Mature follicular dendritic cell networks depend on expression of lymphotoxin β receptor by radioresistant stromal cells and of lymphotoxin β and tumor necrosis factor by B cells. *J. Exp. Med.* 189:159–168.
15. Browning, J.L., and L.E. French. 2002. Visualization of lymphotoxin-beta and lymphotoxin-beta receptor expression in mouse embryos. *J. Immunol.* 168:5079–5087.
16. Murphy, M., B.N. Walter, L. Pike-Nobile, N.A. Fanger, P.M. Guyre, J.L. Browning, C.F. Ware, and L.B. Epstein. 1998. Expression of the lymphotoxin beta receptor on follicular stromal cells in human lymphoid tissues. *Cell Death Differ.* 5:497–505.
17. Futterer, A., K. Mink, A. Luz, M.H. Kosco-Vilbois, and K. Pfeffer. 1998. The lymphotoxin beta receptor controls organogenesis and affinity maturation in peripheral lymphoid tissues. *Immunity.* 9:59–70.
18. Harrop, J.A., P.C. McDonnell, M. Brigham-Burke, S.D. Lyn, J. Minton, K.B. Tan, K. Dede, J. Spampanato, C. Silverman, P. Hensley, et al. 1998. Herpesvirus entry mediator ligand (HVEM-L), a novel ligand for HVEM/TR2, stimulates proliferation of T cells and inhibits HT29 cell growth. *J. Biol. Chem.* 273:27548–27556.
19. Harrop, J.A., M. Reddy, K. Dede, M. Brigham-Burke, S. Lyn, K.B. Tan, C. Silverman, C. Eichman, R. DiPrinzio, J. Spampanato, et al. 1998. Antibodies to TR2 (herpesvirus entry mediator), a new member of the TNF receptor superfamily, block T cell proliferation, expression of activation markers, and production of cytokines. *J. Immunol.* 161:1786–1794.
20. Pakala, S.V., A. Ilic, L. Chen, and N. Sarvetnick. 2001. TNF-alpha receptor 1 (p55) on islets is necessary for the expression of LIGHT on diabetogenic T cells. *Clin. Immunol.* 100:198–207.

21. Chang, Y.H., S.L. Hsieh, Y. Chao, Y.C. Chou, and W.W. Lin. 2005. Proinflammatory effects of LIGHT through HVEM and LTbetaR interactions in cultured human umbilical vein endothelial cells. *J. Biomed. Sci.* 12:363–375.
22. Yu, P., Y. Lee, W. Liu, R.K. Chin, J. Wang, Y. Wang, A. Schietinger, M. Philip, H. Schreiber, and Y.X. Fu. 2004. Priming of naive T cells inside tumors leads to eradication of established tumors. *Nat. Immunol.* 5:141–149.
23. Granger, S.W., and S. Rickert. 2003. LIGHT-HVEM signaling and the regulation of T cell-mediated immunity. *Cytokine Growth Factor Rev.* 14:289–296.
24. Wang, J., R.A. Anders, Q. Wu, D. Peng, J.H. Cho, Y. Sun, R. Karaliukas, H.S. Kang, J.R. Turner, and Y.X. Fu. 2004. Dysregulated LIGHT expression on T cells mediates intestinal inflammation and contributes to IgA nephropathy. *J. Clin. Invest.* 113:826–835.
25. Sedy, J.R., M. Gavrieli, K.G. Potter, M.A. Hurchla, R.C. Lindsley, K. Hildner, S. Scheu, K. Pfeffer, C.F. Ware, T.L. Murphy, and K.M. Murphy. 2005. B and T lymphocyte attenuator regulates T cell activation through interaction with herpesvirus entry mediator. *Nat. Immunol.* 6:90–98.
26. Wang, Y., S.K. Subudhi, R.A. Anders, J. Lo, Y. Sun, S. Blink, J. Wang, X. Liu, K. Mink, D. Degrandi, et al. 2005. The role of herpesvirus entry mediator as a negative regulator of T cell-mediated responses. *J. Clin. Invest.* 115:711–717.
27. Han, P., O.D. Goularte, K. Rufner, B. Wilkinson, and J. Kaye. 2004. An inhibitory Ig superfamily protein expressed by lymphocytes and APCs is also an early marker of thymocyte positive selection. *J. Immunol.* 172:5931–5939.
28. Watanabe, N., M. Gavrieli, J.R. Sedy, J. Yang, F. Fallarino, S.K. Loftin, M.A. Hurchla, N. Zimmerman, J. Sim, X. Zang, et al. 2003. BTLA is a lymphocyte inhibitory receptor with similarities to CTLA-4 and PD-1. *Nat. Immunol.* 4:670–679.
29. Tao, R., L. Wang, R. Han, T. Wang, Q. Ye, T. Honjo, T.L. Murphy, K.M. Murphy, and W.W. Hancock. 2005. Differential effects of B and T lymphocyte attenuator and programmed death-1 on acceptance of partially versus fully MHC-mismatched cardiac allografts. *J. Immunol.* 175:5774–5782.
30. Deppong, C., T.I. Juehne, M. Hurchla, L.D. Friend, D.D. Shah, C.M. Rose, T.L. Bricker, L.P. Shornick, E.C. Crouch, T.L. Murphy, et al. 2006. Cutting edge: B and T lymphocyte attenuator and programmed death receptor-1 inhibitory receptors are required for termination of acute allergic airway inflammation. *J. Immunol.* 176:3909–3913.
31. Krieg, C., O. Boyman, Y.X. Fu, and J. Kaye. 2007. B and T lymphocyte attenuator regulates CD8(+) T cell-intrinsic homeostasis and memory cell generation. *Nat. Immunol.* 8:162–171.
32. Hurchla, M.A., J.R. Sedy, and K.M. Murphy. 2007. Unexpected role of B and T lymphocyte attenuator in sustaining cell survival during chronic allostimulation. *J. Immunol.* 178:6073–6082.
33. Powrie, F. 1995. T cells in inflammatory bowel disease: protective and pathogenic roles. *Immunity.* 3:171–174.
34. Aranda, R., B.C. Sydora, P.L. McAllister, S.W. Binder, H.Y. Yang, S.R. Targan, and M. Kronenberg. 1997. Analysis of intestinal lymphocytes in mouse colitis mediated by transfer of CD4+, CD45RBhigh T cells to SCID recipients. *J. Immunol.* 158:3464–3473.
35. Matsuda, J.L., L. Gapin, B.C. Sydora, F. Byrne, S. Binder, M. Kronenberg, and R. Aranda. 2000. Systemic activation and antigen-driven oligoclonal expansion of T cells in a mouse model of colitis. *J. Immunol.* 164:2797–2806.
36. Morel, Y., A. Truneh, R.W. Sweet, D. Olive, and R.T. Costello. 2001. The TNF superfamily members LIGHT and CD154 (CD40 ligand) costimulate induction of dendritic cell maturation and elicit specific CTL activity. *J. Immunol.* 167:2479–2486.
37. Scheu, S., J. Alferink, T. Potzel, W. Barchet, U. Kalinke, and K. Pfeffer. 2002. Targeted disruption of LIGHT causes defects in costimulatory T cell activation and reveals cooperation with lymphotoxin β in mesenteric lymph node genesis. *J. Exp. Med.* 195:1613–1624.
38. Duhen, T., C. Pasero, F. Mallet, B. Barbarat, D. Olive, and R.T. Costello. 2004. LIGHT costimulates CD40 triggering and induces immunoglobulin secretion; a novel key partner in T cell-dependent B cell terminal differentiation. *Eur. J. Immunol.* 34:3534–3541.
39. Fan, Z., P. Yu, Y. Wang, Y. Wang, M.L. Fu, W. Liu, Y. Sun, and Y.X. Fu. 2006. NK-cell activation by LIGHT triggers tumor-specific CD8+ T-cell immunity to reject established tumors. *Blood.* 107:1342–1351.
40. Heo, S.K., S.A. Ju, S.C. Lee, S.M. Park, S.Y. Choe, B. Kwon, B.S. Kwon, and B.S. Kim. 2006. LIGHT enhances the bactericidal activity of human monocytes and neutrophils via HVEM. *J. Leukoc. Biol.* 79:330–338.
41. Haselmayer, P., S. Tenzer, B.S. Kwon, G. Jung, H. Schild, and M.P. Radsak. 2006. Herpes virus entry mediator synergizes with Toll-like receptor mediated neutrophil inflammatory responses. *Immunology.* 119:404–411.
42. Hurchla, M.A., J.R. Sedy, M. Gavrieli, C.G. Drake, T.L. Murphy, and K.M. Murphy. 2005. B and T lymphocyte attenuator exhibits structural and expression polymorphisms and is highly induced in anergic CD4+ T cells. *J. Immunol.* 174:3377–3385.
43. Murphy, K.M., C.A. Nelson, and J.R. Sedy. 2006. Balancing costimulation and inhibition with BTLA and HVEM. *Nat. Rev. Immunol.* 6:671–681.
44. Shao, L., D. Serrano, and L. Mayer. 2001. The role of epithelial cells in immune regulation in the gut. *Semin. Immunol.* 13:163–176.
45. Cruickshank, S.M., L.D. McVay, D.C. Baumgart, P.J. Felsburg, and S.R. Carding. 2004. Colonic epithelial cell mediated suppression of CD4 T cell activation. *Gut.* 53:678–684.
46. Nakazawa, A., I. Dotan, J. Brimnes, M. Allez, L. Shao, F. Tsushima, M. Azuma, and L. Mayer. 2004. The expression and function of costimulatory molecules B7H and B7-H1 on colonic epithelial cells. *Gastroenterology.* 126:1347–1357.
47. Laouar, A., V. Haridas, D. Vargas, X. Zhinan, D. Chaplin, R.A. van Lier, and N. Manjunath. 2005. CD70+ antigen-presenting cells control the proliferation and differentiation of T cells in the intestinal mucosa. *Nat. Immunol.* 6:698–706.
48. Xu, Y., A.S. Flies, D.B. Flies, G. Zhu, S. Anand, S.J. Flies, H. Xu, R.A. Anders, W.W. Hancock, L. Chen, and K. Tamada. 2007. Selective targeting of the LIGHT-HVEM co-stimulatory system for the treatment of graft-versus-host disease. *Blood.* 109:4097–4104.
49. Fort, M.M., M.W. Leach, and D.M. Rennick. 1998. A role for NK cells as regulators of CD4+ T cells in a transfer model of colitis. *J. Immunol.* 161:3256–3261.
50. Cai, G., A. Anumanthan, J.A. Brown, E.A. Greenfield, B. Zhu, and G.J. Freeman. 2008. CD160 inhibits activation of human CD4+ T cells through interaction with herpesvirus entry mediator. *Nat. Immunol.* 9:176–185.